The polarization effect of a laser in multiphoton Compton scattering*

Liang Guo-Hua(梁国华)†, Lü Qing-Zheng(吕清正), Teng Ai-Ping(滕爱萍), and Li Ying-Jun(李英骏)‡

State Key Laboratory for Geomechanics and Deep Underground Engineer, China University of Mining and Technology, Beijing 100083, *China*

(Received 23 August 2013; revised manuscript received 9 October 2013; published online 18 March 2014)

The multiphoton Compton scattering in a high-intensity laser beam is studied by using the laser-dressed quantum electrodynamics (QED) method, which is a non-perturbative theory for the interaction between a plane electromagnetic field and a charged particle. In order to analyze in the real experimental condition, a Lorentz transformation for the cross section of this process is derived between the laboratory frame and the initial rest frame of electrons. The energy of the scattered photon is analyzed, as well as the cross sections for different laser intensities and polarizations and different electron velocities. The angular distribution of the emitted photon is investigated in a special velocity of the electron, in which for a fixed number of absorbed photons, the electron energy will not change after the scattering in the lab frame. We obtain the conclusion that higher laser intensities suppress few-laser-photon absorption and enhance more-laser-photon absorption. A comparison between different polarizations is also made, and we find that the linearly polarized laser is more suitable to generate nonlinear Compton scattering.

Keywords: multiphoton Compton scattering, laser-dressed quantum electrodynamics (QED), cross section, polarization

PACS: 41.60.–m, 52.25.Os **DOI:** 10.1088/1674-1056/23/5/054103

1. Introduction

Compton scattering is a process that has made people realize that light or electromagnetic waves may have the same particulate nature which belongs to matter.[1] It can be expressed as $e+\omega \rightarrow e'+\omega'$, where e and ω represent the states of electrons and photons before scattering, respectively, while e' and ω' are the corresponding states after scattering. This process can be observed obviously only when the electromagnetic wave is X-ray or γ-ray. Generally, the default Compton scattering refers to the case in which a high energy photon collides with a low energy electron, while the converse situation where an electron with a high speed interacts with an optical photon is called the inverse Compton scattering. In 1929, Klein and Nishina gave the formula for the cross section of this process through calculations based on quantum electrodynamics (QED),[2] in which the Feynman diagram of the interaction between one photon and a free electron was used.

Soon physicists began to investigate the interaction between more photons and one electron, namely, the multiphoton Compton scattering or multiphoton Thomson scattering (the difference between them is whether the quantum effects can be neglected), which can be written as $e+n\omega \rightarrow e'+\omega'$, where n is the number of photons absorbed by the electron. More laser photons participating in the interaction means higher energy photon maybe emitted. In fact, this process is an important way to generate high-energy photon beams experimentally,[3–7] and the corresponding devices are called Compton-based sources of high-energy photons. At present, this kind of source is developing quickly, and has many attractive advantages compared with the synchrotron sources, such as the compactness, tunability, and shortness of photon beams.[8] Such sources, as a helpful experimental device, play an important role in medicine, nuclear physics, and other high-energy process studies.

The nonlinear Compton scattering was firstly observed in the Stanford Linear Accelerator Center (SLAC) in 1996.[9] In that experiment, an about 10^{18} W/cm^2 laser was used, its intensity was already high enough to generate nonlinear optical effects. The spectra of the scattered electrons conformed to the analytical precision[10] within experimental uncertainty, and the absorption of up to 4 photons in one scattering event was also observed. Now, the laser technology is still developing, and the highest laser intensity record is held by the University of Michigan, whose equipment has achieved the intensity of 2×10^{22} W/cm^2.[11,12] This is a very high intensity, although it is still much lower than the critical field intensity $I_c \sim 10^{29}$ W/cm^2 corresponding to an electric field about 1.3×10^{16} V/cm, in which electron–positron pairs would be created spontaneously from the instable vacuum.[13,14] Besides the nonlinear Compton scattering, the high intensity laser generated so far can lead to many other nonlinear quantum effects in experiments, such as pair creation and vacuum polarization.

As a basic nonlinear quantum process, the multiphoton Compton scattering has been investigated in many theoretical

*Project supported by the National Natural Science Foundation of China (Grant No. 11374360) and the National Basic Research Program of China (Grant No. 2013CBA01504).

†Corresponding author. E-mail: xiaolianghmq@gmail.com

‡Corresponding author. E-mail: lyj@aphy.iphy.ac.cn

© 2014 Chinese Physical Society and IOP Publishing Ltd

works,[15–20] especially after the invention of laser. Many of those investigations consider a simple circumstance in which a free electron moves in a plane electromagnetic field, and have derived the formulas for the probability and the cross section of the multiphoton scattering. Those studies may be divided into two kinds according to their methods. One is based on a classical theory and discusses the harmonic generation by derivation from the Hamilton–Jacobi equation. The other is called the laser-dressed QED method, which is used in this paper. In the next section, we will introduce this method.

Experimentally, an electron beam propagates in a laser field instead of a plane wave field. The laser produced in laboratories always needs be focused spatially, so its structure is more complex than that of a plane wave. However, as long as the size of the focusing area is much larger than the main wavelength of the laser pulse, the plane wave approximation is still reasonable. Recently, the shape effects of laser pulses have been investigated numerically,[21,22] and the results show that the effects cannot be neglected only for ultrashort laser pulses. Since the plane wave approximation can give an analytical description of the process, the predictions in this approximation are still important to the multiphoton scattering experiments. In this paper, we assume that the laser pulse is optical and not too short to use the plane wave approximation.

The organization of this paper is as follows. In Section 2, we present a calculation of the cross section for two kinds of polarization conditions and the corresponding kinematic properties, and provide a frame transformation for the cross section in a head-on collision. Section 3 discusses the elastic scattering case, and shows the polarization effects on the angular distribution of the scattered photons. We finally sum up our work in Section 4.

2. Theory and calculation

2.1. Derivation of the cross section

In a high-intensity laser field, the ordinary perturbative QED method is no longer proper for the calculations of quantum processes. An electron which is oscillating in a laser field gets a mean kinetic energy called ponderomotive energy[23] $E_{\rm p}=(\pi e^2 I)/(m_{\rm e}\omega^2)$, where I and ω are the laser intensity and frequency, respectively, and $m_{\rm e}$ is the rest mass of an electron ($\hbar=c=1$ are used throughout this paper). A simple estimation of this energy verifies that $E_{\rm p}$ may equal or even be larger than the electron mass energy $m_{\rm e}c^2$ if a high-intensity laser is employed. The new theory substitutes the eigenstates of an electron in a plane electromagnetic field, namely, the Volkov state,[3,24] for the free particle state, and it is generally shown with a Furry picture.[25]

The electron moving in an electromagnetic field satisfies the Dirac equation

$$(\gamma_\mu {\rm i}\partial^\mu - e\gamma_\mu A^\mu - m)\psi_{\rm p}(x)=0, \tag{1}$$

where A^μ is the four-dimensional vector potential of the field. If the potential depends on the coordinate x only through the scalar product $k\cdot x$, i.e., $A^\mu=A^\mu(k\cdot x)$, where k is the wave vector and $k^2=0$, then the exact solution of this equation can be written as (see Appendix A for details)

$$\psi_{\rm p}(x)=\sqrt{\frac{m}{q^0 V}}\left(1-\frac{e\not{k}\not{A}}{2k\cdot p}\right)u(p,s)\,{\rm e}^{-{\rm i}\Phi-{\rm i}p\cdot x}, \tag{2}$$

here V is the normalization volume, $q^0=p^0-(e^2\langle A^2\rangle k^0)/(2k\cdot p)$, $u(p,s)$ is the unit spinor, and the Feynman notation is used to denote $\not{k}=\gamma^\mu k_\mu$. The phase term Φ can be written as

$$\Phi(k\cdot x)=\int_{-\infty}^{k\cdot x}{\rm d}\varphi\left(\frac{eA(\varphi)\cdot p}{k\cdot p}-\frac{e^2A^2(\varphi)}{2k\cdot p}\right), \tag{3}$$

where the initial condition for the electron is assumed to be $x^0\to-\infty$, $\psi_{\rm p}(x)\sim{\rm e}^{-{\rm i}p\cdot x}$. Note that the form of this solution is for an electron (not a positron), and $e=|e|>0$.

In order to derive the cross section, for simplification, we choose a frame for this process, which is shown in Fig. 1. In this frame, the electron is at rest initially, and the laser propagates along the positive z axis. The polarization vectors parallel to the xy plane, and particularly, there is an angle of $\pi/4$ between the linear polarization vector and the x axis. In this frame, some quantities vanish spontaneously in subsequent computations, such as $p\cdot A$ and $\boldsymbol{p}$, thus it brings many conveniences.

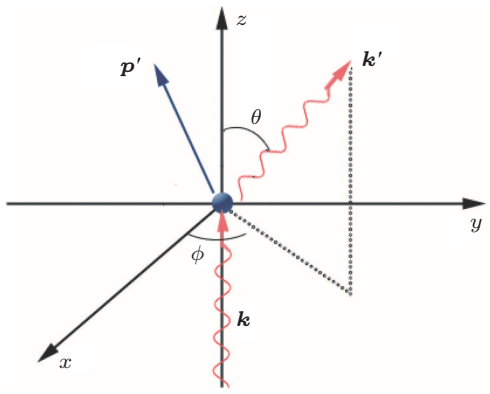


Fig. 1. (color online) The geometry of multiphoton Compton scattering in the frame we choose, where the electron is at rest initially.

It is always useful to express the Volkov state as a Fourier series in calculation, before that, a specific form of the potential must be given. Here, we just give the form of a monochromatic linearly polarized plane wave laser field[26]

$$A_1^\mu=(0,a,a,0)\cos(k\cdot x)=a(\epsilon_1^\mu+\epsilon_2^\mu)\cos(k\cdot x), \tag{4a}$$

and a circularly polarized plane wave laser field[27]

$$A_{\rm c}^\mu=a[\epsilon_1^\mu\cos(k\cdot x)+\epsilon_2^\mu\sin(k\cdot x)], \tag{4b}$$

where a is the amplitude of the vector potential, $\epsilon_1^\mu = (0,1,0,0)$ and $\epsilon_2^\mu = (0,0,1,0)$ are two four-vectors representing the polarization, and the wave vector can be simply written as $k = \omega(1,0,0,1)$. In this way, $\langle A_1^2\rangle = \langle A_c^2\rangle = -a^2$, which means that the two different laser beams have the same intensity.

The amplitude of this scattering process is just the probability with which an electron in state ψ_p transforms into another state $\psi_{p'}$ in the laser field and emits a photon with momentum k' and polarization ϵ', so the amplitude is equal to

$$\begin{aligned}\mathscr{M} &= \langle p's', k'\epsilon', \text{out}|ps, \text{in}\rangle \\ &= -\mathrm{i}e\int \mathrm{d}^4x \mathrm{e}^{\mathrm{i}k'x}\bar{\psi}_{p'}(x)\epsilon'\cdot\gamma\psi_p(x). \end{aligned} \tag{5}$$

Here the radiative correction is neglected.

By regarding the laser field as a plane electromagnetic wave field, the wave functions in expression (5) is the Volkov state. Inserting state (2) into the amplitude, and transforming it into Fourier series (for details see Appendix B), for the linear polarization, we obtain

$$\begin{aligned}\mathscr{M} &= -\mathrm{i}e\frac{m(2\pi)^4}{V\sqrt{q^0q'^0}}\sqrt{\frac{4\pi}{2\omega' V}}\epsilon'_\mu\sum_{n=-\infty}^{\infty}\bar{u}(p',s') \\ &\times\left[\gamma^\mu \mathrm{J}_n - \left(\frac{ea\not{\epsilon}\not{k}\gamma^\mu}{2k\cdot p'} + \frac{ea\gamma^\mu\not{k}\not{\epsilon}}{2k\cdot p}\right)B_n\right. \\ &\left. + \frac{e^2a^2\not{k}k^\mu}{2(k\cdot p')(k\cdot p)}C_n\right]u(p,s)\delta(q-q'-k'+nk), \end{aligned} \tag{6}$$

where $\epsilon = \epsilon_1 + \epsilon_2$, $\mathrm{J}_n = \mathrm{J}_n(\alpha_l, \beta_l)$ is the general Bessel function, which is defined in Eq. (B6) in Appendix B, $B_n = B_n(\alpha_l,\beta_l) = (\mathrm{J}_{n-1}+\mathrm{J}_{n+1})/2$, and $C_n = (\mathrm{J}_{n-2}+2\mathrm{J}_n+\mathrm{J}_{n+2})/4$, with $\alpha_l = eap\cdot(\epsilon_1+\epsilon_2)/(k\cdot p) - eap'\cdot(\epsilon_1+\epsilon_2)/(k\cdot p')$, $\beta_l = e^2a^2/(4k\cdot p') - e^2a^2/(4k\cdot p)$ (these notations will be used from now on). In expression (6), $\delta(q-q'-k'+nk)$ guarantees the four-momentum conservation of the process in which n laser photons are absorbed ($n>0$) or emitted ($n<0$). However, simply taking into account the mass-shell condition $k^2 = 0$ that real photons satisfy relation (B4) in Appendix B, and we find that the process is impossible for $n<1$. From this energy–momentum conservation, we obtain the expression for the emitted photon energy

$$\omega' = \frac{n\omega m}{m + (e^2a^2/(2m) + n\omega)(1-\cos(\theta))}, \tag{7}$$

which is analogous to the Compton's formula.

Then, the rate of this process is given by

$$P = \frac{1}{T}\int\frac{V\mathrm{d}^3q'}{(2\pi)^3}\int\frac{V\mathrm{d}^3k'}{(2\pi)^3}\frac{1}{2}\sum_{\epsilon'}\sum_{\text{spin}}|\mathscr{M}|^2, \tag{8}$$

where T is the interaction time, and a statistic factor 1/2 is included due to the initial spin averaging. Our subsequent calculation mainly focuses on the square term

$$|\mathscr{M}|^2 = \frac{\alpha m^2 T(2\pi)^5}{V^2q^0q'^0\omega'}\sum_{n=1}^{\infty}\mathscr{T}_n\delta(q-q'-k'+nk), \tag{9}$$

where

$$\mathscr{T}_n = [\bar{u}(p,s)\epsilon'^*_\nu\bar{\Gamma}^\nu_n u(p',s')][\bar{u}(p',s')\epsilon'_\mu\Gamma^\mu_n u(p,s)],$$

with

$$\Gamma^\mu_n = \gamma^\mu \mathrm{J}_n - \left(\frac{ea\not{\epsilon}\not{k}\gamma^\mu}{2k\cdot p'} + \frac{ea\gamma^\mu\not{k}\not{\epsilon}}{2k\cdot p}\right)B_n + \frac{e^2a^2\not{k}k^\mu}{2(k\cdot p')(k\cdot p)}C_n,$$

and $\bar{\Gamma}^\nu_n = \gamma^0\Gamma^{\nu\dagger}_n\gamma^0$, here $\alpha = 1/137$ is the fine structure constant, and we have used the replacement rule[28] of

$$\begin{aligned}&\delta(q-q'-k'+nk)\delta(q-q'-k'+n'k) \\ &= \frac{VT}{(2\pi)^4}\delta(q-q'-k'+nk)\delta_{nn'}. \end{aligned} \tag{10}$$

The above rule indicates that in the multiphoton Compton scattering, the absorption of n photons is discrete, in other words, the scattering contains a process of absorbing various integer numbers of photons. Next, we only focus on the term

$$\sum_{\epsilon'}\sum_{\text{spin}}\mathscr{T}_n = \sum_{\epsilon'}\mathrm{Tr}\left(\frac{\not{p}'+m}{2m}\epsilon'_\mu\Gamma^\mu_n\frac{\not{p}+m}{2m}\epsilon'^*_\nu\bar{\Gamma}^\nu_n\right). \tag{11}$$

Before calculating the trace, we may consider the sum of polarization for the emitted photon first. It is convenient to adopt the method of the gauge transformation.[3] Through replacing ϵ' by the gauge invariant quantity

$$\tilde{\epsilon}'_\mu = \epsilon'_\mu - \frac{k\cdot\epsilon'}{k\cdot k'}k'_\mu, \tag{12}$$

the terms with C_n in Γ_n vanish because of $k\cdot\tilde{\epsilon}' = 0$, this will simplify the following work. Certainly, the new polarization sum should be applied, i.e.,

$$\sum_{\epsilon'}(a\cdot\tilde{\epsilon}')(\tilde{\epsilon}'\cdot b) = -a\cdot b + \frac{(a\cdot k)(k'\cdot b)+(a\cdot k')(k\cdot b)}{k\cdot k'}. \tag{13}$$

Computing the trace in consideration of Eq. (13), we obtain

$$\sum_{\epsilon'}\sum_{\text{spin}}\mathscr{T}_n = \frac{1}{m^2}[E_l|\mathrm{J}_n|^2 + F_l\mathrm{Re}(\mathrm{J}_nB_n) + G_l|B_n|^2], \tag{14a}$$

where $E_l = -2m^2 + (p\cdot k')H$, $F_l = ea(k'\cdot A)H$, $G_l = e^2a^2k\cdot k'H/(p\cdot k)$ with $H = (p\cdot k + p'\cdot k)^2/((p'\cdot k)(k\cdot k'))$, and all the subscripts l denote the linearly polarized laser field.

For a circularly polarized laser field, the analogous term becomes

$$\sum_{\epsilon'}\sum_{\text{spin}}\mathscr{T}_n = \frac{1}{m^2}[E_c|\mathrm{D}_n|^2 + G_c(|\mathrm{D}_{n-1}|^2 + |\mathrm{D}_{n+1}|^2)], \tag{14b}$$

where $E_c = E_l$, $G_c = G_l/2$, $\mathrm{D}_n = \mathrm{D}_n(\xi - \xi')$ is the ordinary Bessel function with $\xi - \xi' = -ea\sqrt{(p'\cdot\epsilon_1)^2 + (p'\cdot\epsilon_2)^2}/(p'\cdot k)$, and subscript c denotes the circularly polarized laser field.

Comparing Eq. (14a) with Eq. (14b), we find that in the circular case, the middle term which is similar to F_1 vanishes. This is expected because F_1 is the only term with a dependence on ϕ in Eq. (14b) except the general Bessel functions, and the circularly polarized laser has a symmetry that in all ϕ directions, the potential has the same amplitude, so this term should only appear in the linear case, which does not have this symmetry. Besides the symmetry, the main difference of the two polarizations in the scattering process is reflected in the two kinds of Bessel functions. The E_1, G_1 and E_c, G_c are clearly considered as the kinematic terms.

When calculating the differential cross section of this process

$$\frac{\mathrm{d}\sigma}{\mathrm{d}\Omega_{k'}} = \frac{1}{\rho}\frac{\mathrm{d}P}{\mathrm{d}\Omega_{k'}}, \tag{15}$$

we shall just consider the case of absorbing n photons. In view of $\int \mathrm{d}^3k' = \int \omega'^2 \mathrm{d}\omega' \mathrm{d}\Omega_{k'}$, substituting Eq. (8) in relation (15) yields

$$\begin{aligned}\frac{\mathrm{d}\sigma_n}{\mathrm{d}\Omega_{k'}} &= \frac{\alpha m^2}{4\pi\rho q^0 q'^0}\int \mathrm{d}\omega'\omega' \sum_{\epsilon'}\sum_{\text{spin}} \mathscr{T}_n \\ &\quad \times \delta\left(\omega' - n\omega - \frac{e^2a^2}{2m} + \sqrt{|\boldsymbol{q}'|^2 + m_*^2}\right) \\ &= \frac{\alpha\omega'^2}{2\pi\rho n\omega(2+\eta^2)}\sum_{\epsilon'}\sum_{\text{spin}} \mathscr{T}_n, \end{aligned} \tag{16}$$

where $m_* = \sqrt{m^2 + e^2a^2}$ is called the effective mass, and the dimensionless Lorentz-invariant parameter $\eta = e\sqrt{-\langle A_\mu A^\mu\rangle}/m = ea/m$ is used, which characterizes the work, in contrast with the electron rest energy that the electromagnetic field imposes on the particle over a wavelength. Apparently, this parameter is a denotation of the laser intensity. And ρ is the flux of the incident photon beam, which may be calculated in the following way:

$$\rho = \frac{N_{\text{photons}}}{V} = \frac{I_{\text{laser}}V}{\omega V} = \frac{\omega^2\langle A^2\rangle}{4\pi\omega} = \frac{\omega m^2\eta^2}{4\pi\alpha}, \tag{17}$$

here V is the volume containing N photons in the laser field.

So far, we have derived the differential cross section of the n photons Compton scattering for both linearly and circularly polarized lasers. Reviewing the expressions about the cross sections, especially Eqs. (14a) and (14b), we find that the cross sections are dependent on the laser intensity. This is different from the case in a weak field and shows the nonlinear effects of the strong field.

2.2. Transformation between the initial rest frame and the laboratory frame

In the previous subsection, for simplification, we derive the formula in the frame in which the electrons are initially at rest. We call this frame the R frame. However, in the laboratory, the electron beams are always accelerated to relativistic speeds. In order to analyze the real experiment and give some predictions, we need to transform our formula to the laboratory frame, namely, the L frame.

If an electron moves with speed $-v$ in the L frame, two formulae are workable for light, namely,

$$\omega'_{\text{R}}(\theta_{\text{R}}) = \omega'_{\text{L}}(\theta_{\text{L}})\gamma_{\text{D}}(1 - \beta_{\text{D}}\cos\theta_{\text{L}}), \tag{18}$$

$$\cos\theta_{\text{R}} = \frac{\cos\theta_{\text{L}} - \beta_{\text{D}}}{1 - \beta_{\text{D}}\cos\theta_{\text{L}}}, \tag{19}$$

where $\beta_{\text{D}} = -v/c$ and $\gamma_{\text{D}} = 1/\sqrt{1-\beta_{\text{D}}^2}$.

Next we shall consider the transformation of the cross section, that is

$$\frac{\mathrm{d}\sigma_{\text{L}}}{(\mathrm{d}\Omega_{k'})_{\text{L}}} = \frac{\rho_{\text{R}}}{\rho_{\text{L}}}\frac{(\mathrm{d}\Omega_{k'})_{\text{R}}}{(\mathrm{d}\Omega_{k'})_{\text{L}}}\frac{T_{\text{R}}}{T_{\text{L}}}\frac{\mathrm{d}\sigma_{\text{R}}}{(\mathrm{d}\Omega_{k'})_{\text{R}}}. \tag{20}$$

This differential transformation is easily achieved with the help of Eqs. (18) and (19). Then, we can sum up and give a briefer expression for the differential cross section in the L frame

$$\frac{(\mathrm{d}\sigma_n)_{\text{L}}}{(\mathrm{d}\Omega_{k'})_{\text{L}}} = N_{\text{D}}N_{\text{R}}\pi r_{\text{e}}^2 \sum_{\epsilon'}\sum_{\text{spin}} \mathscr{T}_n, \tag{21}$$

with

$$\begin{aligned} N_{\text{D}} &= \gamma_{\text{D}}^2(1+\beta_{\text{D}})(1+\beta_{\text{D}}\cos\theta_{\text{R}})^2, \\ N_{\text{R}} &= \frac{2\omega'^2_{\text{R}}}{\pi\eta^2 n\omega_{\text{R}}^2(2+\eta^2)}, \end{aligned}$$

where $r_{\text{e}} = \alpha/m$ is the classical electron radius. Hence, knowing the cross section at the angle position $(\theta_{\text{R}}, \phi)$ in the R frame, we can easily obtain the corresponding quantity at the angle position $(\theta_{\text{L}}, \phi)$ in the L frame.

3. Investigation on the polarization effects

Let us first concentrate on the dependence of ω'_{L} on θ_{L}. To obtain an explicit representation of the relationship, we should consider expressions (7), (18), and (19) overall and perform some substitutions. Then it is straightforward to obtain $\mathrm{d}\omega'_{\text{L}}/\mathrm{d}\theta_{\text{L}}$, if let it be 0, we can find an interesting and special value of β_{D}, that is

$$\beta_{\text{s}} = \frac{-v_{\text{s}}}{c} = -\frac{m\eta^2 + 2n\omega_{\text{R}}}{m\eta^2 + 2n\omega_{\text{R}} + 2m} = -\frac{|\boldsymbol{q}_{\text{R}}| + n|\boldsymbol{k}_{\text{R}}|}{q^0_{\text{R}} + nk^0_{\text{R}}}. \tag{22}$$

For a fixed n, if $\beta_{\text{D}} > \beta_{\text{s}}$, $\omega'_{\text{L}}(\theta_{\text{L}})$ decreases with θ_{R} or θ_{L} increasing from 0 to π, however, if $\beta_{\text{D}} < \beta_{\text{s}}$, the case will be opposite, and if $\beta_{\text{D}} = \beta_{\text{s}}$, $\omega'_{\text{L}}(\theta_{\text{L}})$ will be the same in all directions and the accurate value of the energy of the scattered photon in the L frame is $\omega'_{\text{s}} = n\omega$ (see Fig. 2). It means that in this case, the energy of an electron will not change after the scattering no matter where the electron is scattered to. In Fig. 2, the energies of the emitted photons from front scattering ($\theta = 0^\circ$) and back scattering ($\theta = 180^\circ$) with different initial electron

velocities are showed. The energy of the scattered photon in the front scattering changes little no matter how fast the electron moves, while in the back scattering, the energy increases quickly when the speed of the electron beam approaches to $-c$. In the figure, the position where $\omega'_{\rm L}(\theta=0^\circ)=\omega'_{\rm L}(\theta=180^\circ)$ is just at $\beta_{\rm D}=\beta_{\rm s}$. We may call this the elastic scattering case, since it is just like the elastic Compton scattering. Considering in the L frame and substituting the relation between $\omega_{\rm R}$ and $\omega_{\rm L}$ into the expression of $\beta_{\rm s}$, we may have

$$\beta_{\rm s}=\frac{-m^2(2\eta^2+\eta^4)-4n\omega_{\rm L}\sqrt{(1+\eta^2)m^2+n^2\omega_{\rm L}^2}}{m^2(2+\eta^2)^2+4n^2\omega_{\rm L}^2}.$$

If the laser source used in lab is optical and intense, namely, $\omega_{\rm L}\ll m$ and $\eta\sim 1$, and n is not very large, the parameter can be simply written as $\beta_{\rm s}\sim -\eta^2/(2+\eta^2)$, so this velocity is mainly determined by the laser strength in this condition.

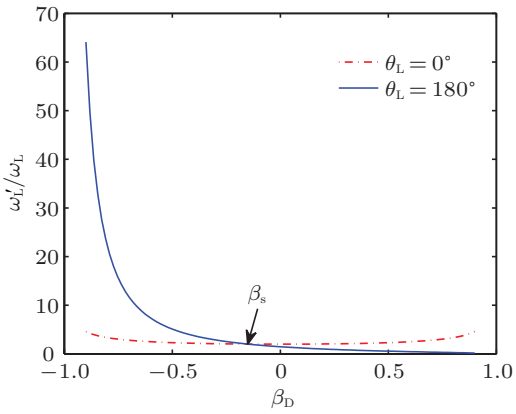


Fig. 2. (color online) Dependence of ratio $\omega'_{\rm L}/\omega_{\rm L}$ on $\beta_{\rm D}$ at $\theta=0^\circ$ and $\theta=180^\circ$ in the scattering process of 2-photon absorption ($\eta=0.6$, which corresponds to the laser intensity of 10^{18} W/cm^2, $\lambda=1054$ nm). Note that $\beta_{\rm D}<0$ when the electron moves along the negative z axis. The intersection of the two curves is located at position $(\beta_{\rm s},2)$.

Moreover, noting that $\beta_{\rm D}$ always has the form $|\boldsymbol{p}|/p^0$ and taking note of the right side of Eq. (22), we may have the relation

$$(|\boldsymbol{q}_{\rm R}|+n|\boldsymbol{k}_{\rm R}|)^2+m_{\rm s}^2=(q_{\rm R}^0+nk_{\rm R}^0)^2, \tag{23}$$

and it is easy to find that $m_{\rm s}=\sqrt{m_*^2+2nm\omega_{\rm R}}$. Hence inspired by the elastic scattering case, the scattering with n-photon absorption can be viewed as a process in which an unstable particle whose mass is $m_{\rm s}$ decays into a photon and an electron with the Volkov state. It is worthwhile to note that the decay process in this case gives a relatively symmetrically angular distribution of the cross section which will be shown later, and more details of the interaction between photons and electrons can be reflected.

From the discussion in Section 2, we find that the main difference in the angular distribution of the cross section between the two kinds of polarized fields should appear in the ϕ direction. However, we investigate the $\theta_{\rm L}$ direction first. Particularly, the electron velocity is chosen to be that in the elastic scattering case. The reason has been given before. Figure 3 shows the angular distribution (at the $\theta_{\rm L}$ direction) of the emitted photons in multiphoton Compton scattering in linearly ($\phi=45^\circ$) and circularly polarized laser fields.

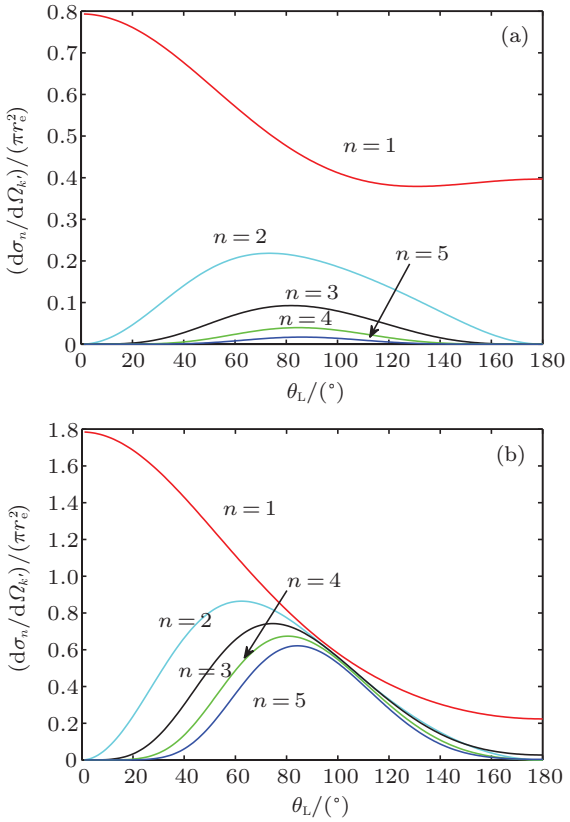


Fig. 3. (color online) The angular distribution of the cross section (scaled by $\pi r_{\rm e}^2$) of the scattering for different numbers of absorbed photons with (a) circular polarization and (b) linear polarization in the L frame. All curves are plotted for the elastic scattering case, and $\eta=0.6$, $\lambda=1054$ nm.

It is shown in Fig. 3 that if the electron moves with speed $\beta_{\rm s}c$ and $\omega_{\rm L}\ll m$, the maximum position of the cross section approaches $\theta_{\rm L}=90^\circ$ with n increasing for both circular and linear polarization cases. For $n=1$, the maximum always appears at $\theta_{\rm L}=0^\circ$, which agrees with the K–N formula. However for $n>1$, the maximum positions are all between $\theta_{\rm L}=0^\circ$ and $\theta_{\rm L}=180^\circ$, and the cross section decreases to zero when $\theta_{\rm L}$ tends to 0° and 180°. The outstanding distinctions between curves for $n=1$ and $n>1$ indicate that the multiphoton Compton scattering has an intrinsically different process in contrast with the one-photon Compton scattering. To understand this difference, we should go back to expression (21). As in the elastic scattering case, $0.1<\beta_{\rm D}<0.2$, $N_{\rm D}$ has little influence on the angular distribution in Fig. 3. So the main difference comes from the term $\sum_{\epsilon'}\sum_{\rm spin}\mathscr{T}_n$. Equations (14a) and (14b) give the expressions of this term for linear and circular polarization cases. We mainly analyze the behavior of the Bessel

functions. For the ordinary Bessel function $\mathrm{D}_n(\xi-\xi')$, neglecting the constant phase $\mathrm{e}^{-\mathrm{i}n\pi/4}$, we can express it in another form, namely,

$$\mathrm{D}_n(\xi-\xi')=\frac{\xi-\xi'}{2}\sum_{k=0}^{\infty}\frac{(-1)^k((\xi-\xi')/2)^{2k}}{k!(n+k)!}.$$

When $\theta_\mathrm{L}\to 0^\circ$ and 180°, $\xi-\xi'\to 0$. It is clear that every D_n with $n>0$ vanishes, however, $\mathrm{D}_0(0)=1$. So the key difference between the one-photon and the multiphoton Compton scatterings in a circularly polarized field is that the former contains a zero order Bessel function. It is analogous to analyze the linear polarization case. Considering the condition $n\omega_\mathrm{L}\ll m$, we find $\alpha_\mathrm{l}\to 0$ and $\beta_\mathrm{l}\sim 0$ when $\theta_\mathrm{L}\to 0^\circ$ and 180°. For $n\geq 0$, we have the following Taylor expansions of the general Bessel functions in Eq. (14a):

$$\mathrm{J}_n(\alpha_\mathrm{l},\beta_\mathrm{l})=\delta_{n0}+\frac{\alpha_\mathrm{l}}{2}\delta_{n1}-\frac{\beta_\mathrm{l}}{2}\delta_{n2}+\mathrm{O}(\alpha_\mathrm{l}^2,\beta_\mathrm{l}^2),$$

$$B_n(\alpha_\mathrm{l},\beta_\mathrm{l})=\frac{1}{2}\left[\delta_{n1}+\frac{\alpha_\mathrm{l}}{2}\delta_{n2}-\frac{\beta_\mathrm{l}}{2}(\delta_{n1}+\delta_{n3})\right]+\mathrm{O}(\alpha_\mathrm{l}^2,\beta_\mathrm{l}^2),$$

here δ_{ij} is Kronecker's delta function. Then we can also discover that the nonzero term $\mathrm{J}_0(0,0)$ or $B_1(0,0)$ is included only for the one-photon Compton scattering. Therefore, the zero order Bessel functions signify the process of the one-photon Compton scattering.

From the figure, we can see that the cross sections decrease with n increasing no matter where we observe. However the cross sections for $n=1,\ldots,5$ have the same order of magnitude. This is totally different from the Compton scattering in a weak field and obviously is a reflection of the nonlinear effect of a strong laser field. The figures also suggest that we can use the maximum of the differential cross section $\mathrm{d}\sigma_n$ to represent the total cross section σ_n roughly in such an elastic scattering case. However, further calculations show that if the intensity is even higher, the conclusion is not right for the linear polarization field.

To find the approximate maximums of lines in Fig. 3, we set $\theta_\mathrm{L}=60^\circ$ for $n=2$, $\theta_\mathrm{L}=70^\circ$ for $n=3$, and $\theta_\mathrm{L}=80^\circ$ for $n=4$, besides, we set $\theta_\mathrm{L}=30^\circ$ for $n=1$ as a comparison. In Fig. 4, we plot the dependence of the cross section corresponding to different polarized laser on the azimuth angle ϕ in the polar coordinate, and we still choose $\beta_\mathrm{s}c$ as the electron velocity. The potential with circular polarization has a symmetry in the ϕ direction, so the corresponding distribution of the differential cross section form a circle in the polar coordinate.

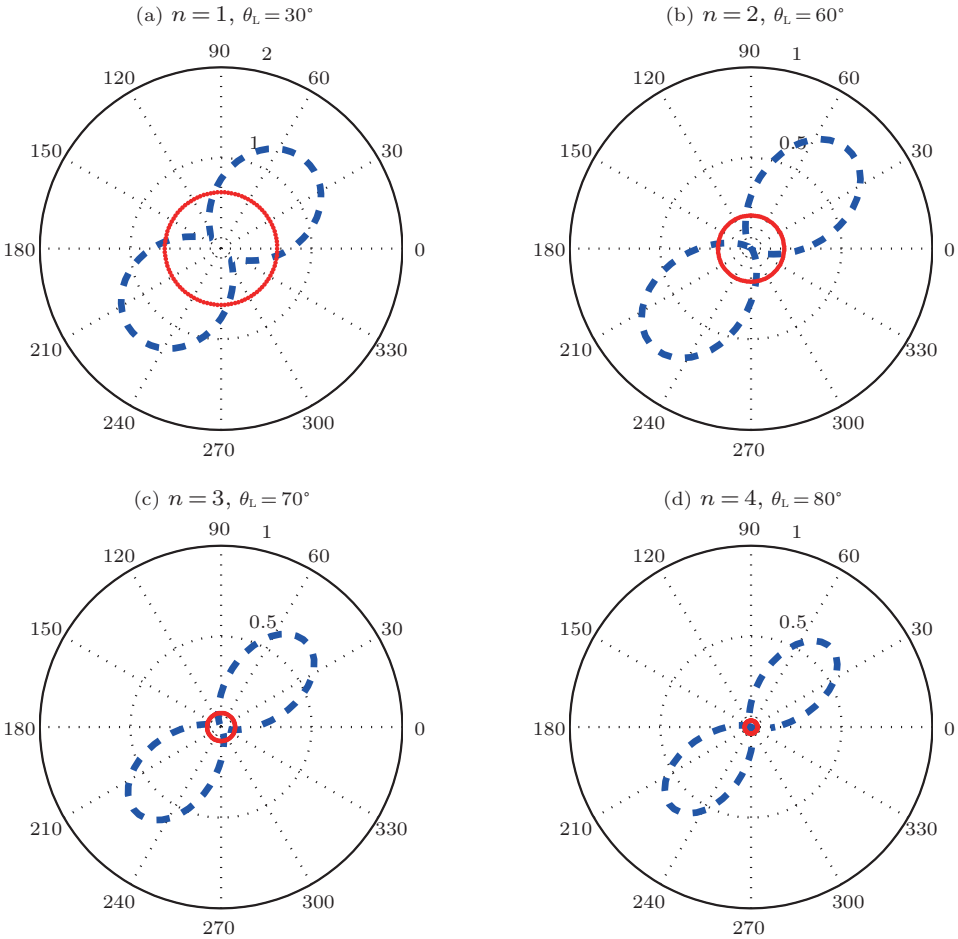


Fig. 4. (color online) The dependence of the cross section (scaled by πr_e^2) corresponding to different polarized laser on the azimuth angle ϕ in the polar coordinate, where (a) $\theta_\mathrm{L}=30^\circ$, (b) $\theta_\mathrm{L}=60^\circ$, (c) $\theta_\mathrm{L}=70^\circ$, and (d) $\theta_\mathrm{L}=80^\circ$ correspond to $n=1,2,3,4$, respectively. Note that the radius of the first figure is twice of that in the other figures. The red circles indicate the cross sections for the circular polarization, and the blue dash lines show the linear polarization cases.

In contrast, the angular distribution for the linearly polarized laser field in this coordinate forms a figure like an "8" (see blue dash lines in Fig. 4.), which has two symmetry axes. Comparing the four figures one by one, we can easily find that the areas surrounded by the red circles decrease more quickly than the ones surrounded by the blue lines with increasing n, and this is especially obvious for the figures of $n = 2,3,4$. This phenomenon indicates a fact that a linearly polarized laser generates higher harmonics better than a circular one.

We still have to focus on the characters of the angular distribution of the emitted photons in the ϕ direction for the linearly polarized field. In Fig. 5, we copy the angular distributions for the linear polarization with $n = 1,2,3$ and plot them in the same place, we also plot the case of $n = 10$ with $\theta_L = \pi/2$. From this figure, we can conclude that for a fixed θ_L, the cross sections of the multiphoton Compton scattering in the linearly polarized laser have maximums at its polarization direction, namely, $\phi = \pi/4$ and $\phi = 5\pi/4$, and minimums at the direction orthogonal to its polarization direction, that is $\phi = 3\pi/4$ and $\phi = 7\pi/4$. Another conclusion obtained from the figure is that for the linearly polarized laser, the more laser photons are absorbed, the better directivity the scattered photons have in the ϕ direction, since the shapes are getting thinner with n increasing. This is a good sign for the design of light sources.

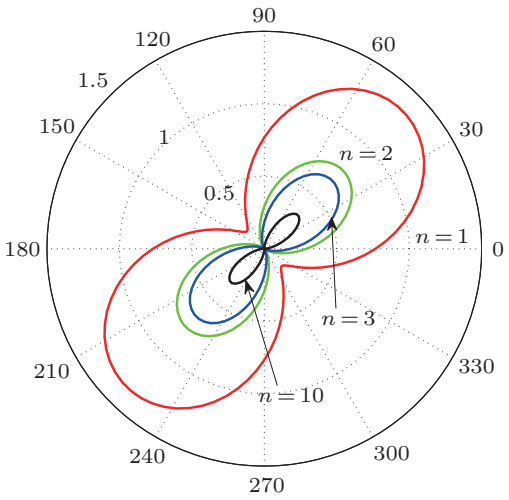


Fig. 5. (color online) The dependence of the cross section (scaled by πr_e^2) corresponding to the linear polarized laser on the azimuth angle ϕ in the polar coordinate. The lines of $n = 1,2,3$ are the same as the corresponding blue dashed lines in Fig. 4, and the line of $n = 10$ is drawn when $\theta_L = 90°$.

A conclusion that higher laser intensities suppress low-order harmonics and enhance higher-order harmonics was drawn in Ref. [29], in which the scattering process was calculated in a classical way. It is necessary to check if this conclusion is right for both linearly and circularly polarized laser fields. In Fig. 6, we plot the cross section versus η for different n, with observation angle $\theta_L = \pi/2$, initial electron velocity $v_e = \beta_s c$, and laser wave length $\lambda = 1054$ nm. From this figure, we find the maximums of the cross sections shift to right with n increasing, and this is especially obvious for the linear polarization case (see Fig. 6(b)). This implies that every n-photon scattering process has its appropriate laser intensity, and this intensity raises with n increasing. Therefore, the conclusion is verified.

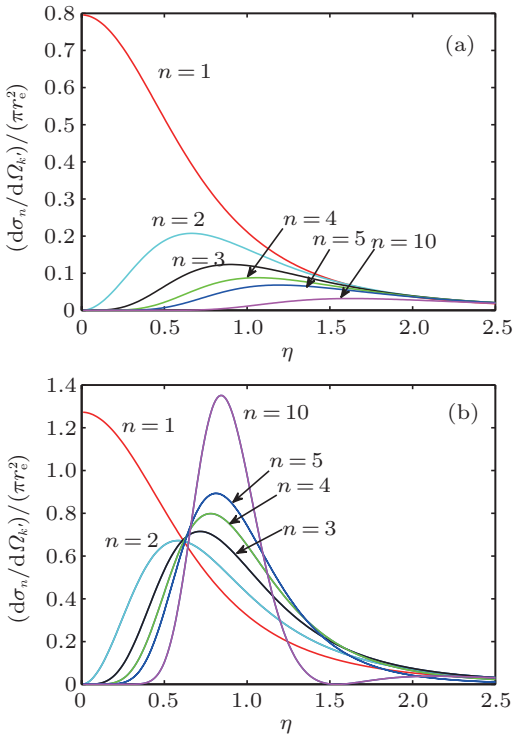


Fig. 6. (color online) The cross section for n-photon scattering in a circularly polarized laser field is plotted against the intensity parameter η. All curves correspond to observation angle $\theta_L = \pi/2$, electron velocity $\beta_s c$, and laser wave length $\lambda = 1054$ nm. Panles (a) and (b) are for the circular polarization and the linear laser polarization ($\phi = 45°$), respectively.

Furthermore, different from the circular case, all curves in Fig. 6(b) have maximums at the intensity approaching $\eta \sim 1$ and the values even have a little increase when n increases. This may because at such a high intensity, the emitted photon from a larger n-photon absorption channel is more likely to gather to the area where the max differential cross section appears. It can also be explained from the above discussion about inhomogeneous angular distribution.

4. Summary and outlook

From the derivation, we know that besides the two different kinds of Bessel functions, the cross-section formula of the multiphoton Compton scattering for the linearly polarized laser field has an extra term compared with the circular one. The extra term, as well as the general Bessel function, gives an asymmetry for the angular distribution of the emitted photons in the ϕ direction.

We find an elastic scattering case in which the initial velocity of an electron in the laboratory frame is $\beta_s c$, and the generated photon has the energy of $n\omega_L$ no matter where it goes, for a fixed n. The angular distribution of the cross section for this velocity is investigated when $\eta \sim 1$ and $\omega_L \ll m$, and the maximum approaching to $\theta_L = \pi/2$ is discovered. We have shown a pictorial comparison between linearly and circularly polarized lasers in the scattering process, and obtained an impression that the linearly polarized light supports the multiphoton Compton scattering better than the circular one. For a fixed θ_L, the linear polarization case has a maximum cross section at the direction parallel to its polarization when the number of absorbed photons is not big. Moreover, the conclusion that higher laser intensities suppressed low-order harmonics and enhanced higher-order harmonics is also verified.

Acknowledgment

The authors wish to thank Dr. Hu Hua-Yu for her many useful comments and help.

Appendix A

We need to solve Dirac equation (1) with condition $A^\mu = A^\mu(\varphi = k\cdot x)$ and $k^2 = 0$. The four-potential A^μ satisfies the Lorentz gauge condition, that is $\partial_\mu A^\mu = k\cdot \mathrm{d}A/\mathrm{d}\varphi = 0$, which implies $k\cdot A = 0$.

To find the solution, it is helpful to turn to the second-order Dirac equation

$$(\gamma_\mu \mathrm{i}\partial^\mu - e\gamma_\mu A^\mu + m)(\gamma_\nu \mathrm{i}\partial^\nu - e\gamma_\nu A^\nu - m)\psi_p(x) = 0. \quad \text{(A1)}$$

Using Dirac matrices property $\{\gamma_\mu, \gamma_\nu\} = 2g_{\mu\nu}$ and the definition $\sigma_{\mu\nu} = \mathrm{i}[\gamma_\mu, \gamma_\nu]/2$, we rewrite this equation as

$$\left(\Pi^2 - m^2 + \frac{1}{2}e\sigma_{\mu\nu}F^{\mu\nu}\right)\psi_p(x) = 0, \quad \text{(A2)}$$

where $\Pi_\mu = \mathrm{i}\partial_\mu - eA_\mu$, and $F^{\mu\nu} = \partial^\mu A^\nu - \partial^\nu A^\mu$ is the tensor electromagnetic field. Furthermore, thanks to $\partial_\mu A^\mu = 0$, the equation has the form

$$\left(-\partial^2 - 2\mathrm{i}eA\cdot\partial + e^2A^2 - m^2 - \mathrm{i}e\not{k}\frac{\mathrm{d}\not{A}}{\mathrm{d}\varphi}\right)\psi_p(x) = 0. \quad \text{(A3)}$$

Simply analyzing this equation, we can realize that the solution should be in the form

$$\psi_p(x) = \mathrm{e}^{-\mathrm{i}p\cdot x}F(\varphi). \quad \text{(A4)}$$

By noticing $\partial^2 F(\varphi) = k^2\partial^2 F/\partial\varphi^2 = 0$ and $p^2 = m^2$, the equation for $F(\varphi)$ becomes much easier, namely,

$$2\mathrm{i}k\cdot p\frac{\partial F}{\partial\varphi} = \left(2ep\cdot A - e^2A^2 + \mathrm{i}e\not{k}\frac{\partial\not{A}}{\partial\varphi}\right)F. \quad \text{(A5)}$$

The integral of this equation gives

$$F = \exp\left[-\mathrm{i}\int_{-\infty}^{k\cdot x}\left(\frac{ep\cdot A}{pk} - \frac{e^2A^2}{2p\cdot k}\right)\mathrm{d}\varphi + \frac{e\not{k}\not{A}}{2p\cdot k}\right] \times u(p,s), \quad \text{(A6)}$$

where $u(p,s)$ is a constant spinor, and here we assume the initial condition is $F \to u(p,s)$ as $k\cdot x \to -\infty$. In the particular case where $A \to 0$, $u(p,s)$ is identified as an electron spinor satisfying the free Dirac equation $(\not{p} - m)u(p,s) = 0$.

Since $\not{k}\not{A}\not{k}\not{A} = -k^2A^2 + 2k\cdot A\not{k}\not{A} = 0$, then we have

$$\exp\left(\frac{e\not{k}\not{A}}{2p\cdot k}\right) = 1 + \frac{e\not{k}\not{A}}{2p\cdot k}.$$

Finally, we can write the solution in the form

$$\psi_p(x) = N\left(1 + \frac{e\not{k}\not{A}}{2p\cdot k}\right)u(p,s)\,\mathrm{e}^{-\mathrm{i}p\cdot x - \mathrm{i}\Phi}, \quad \text{(A7)}$$

where

$$\Phi(k\cdot x) = \int_{-\infty}^{k\cdot x}\left(\frac{ep\cdot A}{p\cdot k} - \frac{e^2A^2}{2p\cdot k}\right),$$

and N is a normalization constant. To determine the constant N, a box normalization can be imposed. Assume the normalization volume is V, which means

$$\rho V = \langle j^0\rangle V = 1, \quad \text{(A8)}$$

where

$$\langle j^0\rangle = \langle\bar\psi_p\gamma^0\psi_p\rangle = N^2\frac{1}{m}\left(p^0 - \frac{e^2\langle A^2\rangle}{2k\cdot p}k^0\right) = N^2\frac{q^0}{m}$$

is the mean value a component of the Dirac current density. Then the normalization constant is $N = \sqrt{m/q^0V}$.

In addition, its orthonormalization

$$\int \mathrm{d}^3x\psi^\dagger_{p,s}(x)\psi_{p',s'}(x) = (2\pi)^3\delta(\boldsymbol{p} - \boldsymbol{p}')\delta_{ss'} \quad \text{(A9)}$$

and completeness

$$\int \mathrm{d}^3p\sum_{s=1}^{4}\psi^\dagger_{p,s}(\boldsymbol{x},t)\psi_{p,s}(\boldsymbol{x}',t) = (2\pi)^3\delta(\boldsymbol{x} - \boldsymbol{x}')I \quad \text{(A10)}$$

have been proven,[30] where I is the four by four unit matrix.

Appendix B

To obtain the Fourier form of the Volkov state, we need to simplify the phase term. Substituting these two potentials to phase term (4), we obtain

$$\Phi_c = \frac{e^2a^2}{2k\cdot p}k\cdot x - \frac{eap\cdot\epsilon_1}{k\cdot p}\sin(k\cdot x) + \frac{eap\cdot\epsilon_2}{k\cdot p}\cos(k\cdot x), \quad \text{(B1)}$$

$$\Phi_l = \frac{e^2a^2}{2k\cdot p}k\cdot x - \frac{eap\cdot(\epsilon_1+\epsilon_2)}{k\cdot p}\sin(k\cdot x) + \frac{e^2a^2}{4k\cdot p}\sin(2k\cdot x). \quad \text{(B2)}$$

The first term in the two phases can be absorbed into quantity

$$q\cdot x=\left(p+\frac{e^2a^2}{2k\cdot p}k\right)\cdot x,$$

and

$$q^\mu=p^\mu+\frac{e^2a^2}{2k\cdot p}k^\mu \tag{B3}$$

is defined as an effective momentum. There is also an analogous mass shell relation

$$q^2=m_*^2=m^2\left(1+\frac{e^2a^2}{m^2}\right), \tag{B4}$$

with m_* called the effective mass.

Now, it is straightforward to write the Fourier form of the state. For the linearly polarized laser field,

$$\begin{aligned}\psi_{\rm p}(x) &= \sqrt{\frac{m}{q^0V}}\left(1-\frac{e\not{k}\not{A}}{2k\cdot p}\right)u(p,s)\,{\rm e}^{-{\rm i}q\cdot x}\\ &\quad\times\sum_{n=-\infty}^{\infty}{\rm J}_n(\alpha_{\rm p},\beta_{\rm p})\,{\rm e}^{{\rm i}nk\cdot x}\\ &= \sqrt{\frac{m}{q^0V}}u(p,s)\,{\rm e}^{-{\rm i}q\cdot x}\sum_{n=-\infty}^{\infty}\Big[{\rm J}_n(\alpha_{\rm p},\beta_{\rm p})\\ &\quad-\frac{ea\not{k}\not{\epsilon}}{2k\cdot p}B_n(\alpha_{\rm p},\beta_{\rm p})\Big]\,{\rm e}^{{\rm i}nk\cdot x},\end{aligned} \tag{B5}$$

with

$$\alpha_{\rm p}=\frac{eap\cdot(\epsilon_1+\epsilon_2)}{k\cdot p},\quad \beta_{\rm p}=-\frac{e^2a^2}{4k\cdot p},$$

and

$$B_n(\alpha_{\rm p},\beta_{\rm p})=\frac{1}{2}[{\rm J}_{n-1}(\alpha_{\rm p},\beta_{\rm p})+{\rm J}_{n+1}(\alpha_{\rm p},\beta_{\rm p})],$$

where ${\rm J}_n(\alpha_{\rm p},\beta_{\rm p})$ is the generalized Bessel function, which can be given in the integral representation as[31,32]

$$\begin{aligned}&{\rm J}_n(\alpha_{\rm p},\beta_{\rm p})\\ &=\frac{1}{2\pi}\int_{-\pi}^{\pi}\exp[-{\rm i}n\theta+{\rm i}\alpha_{\rm p}\sin\theta+{\rm i}\beta_{\rm p}\sin2\theta]\,{\rm d}\theta.\end{aligned} \tag{B6}$$

For the circularly polarized laser field,

$$\begin{aligned}&\psi_{\rm p}(x)\\ &=\sqrt{\frac{m}{q^0V}}u(p,s)\,{\rm e}^{-{\rm i}q\cdot x}\sum_{n=-\infty}^{\infty}{\rm e}^{{\rm i}nk\cdot x}\\ &\quad\times\left[{\rm D}_n(\xi)-\frac{eak\!\!\!/\gamma_\mu}{2k\cdot p}\left(\epsilon_-^\mu{\rm D}_{n-1}(\xi)+\epsilon_+^\mu{\rm D}_{n+1}(\xi)\right)\right],\end{aligned} \tag{B7}$$

with

$$\begin{aligned}\epsilon_-^\mu&=\frac{\epsilon_1^\mu-{\rm i}\epsilon_2^\mu}{2},\\ \epsilon_+^\mu&=\frac{\epsilon_1^\mu+{\rm i}\epsilon_2^\mu}{2},\\ \xi&=\frac{ea}{k\cdot p}\sqrt{(p\cdot\epsilon_1)^2+(p\cdot\epsilon_2)^2},\\ {\rm D}_n(\xi)&=\frac{1}{2\pi}\int_{-\pi}^{\pi}\exp\Big[-{\rm i}n\theta+{\rm i}\frac{eap\cdot\epsilon_1}{k\cdot p}\sin(\theta)\\ &\quad-{\rm i}\frac{eap\cdot\epsilon_2}{k\cdot p}\cos(\theta)\Big]\,{\rm d}\theta={\rm D}_n(\xi)\,{\rm e}^{-{\rm i}n\pi/4},\end{aligned} \tag{B8}$$

where ${\rm D}_n(\xi)$ is the ordinary Bessel function. Besides, there is a mathematical relation between these two functions

$${\rm J}_n(\alpha_{\rm p},\beta_{\rm p})=\sum_{l=-\infty}^{\infty}{\rm D}_{n-2l}(\alpha_{\rm p}){\rm D}_l(\beta_{\rm p}), \tag{B9}$$

and it provides a way to obtain the approximate value of a general Bessel function.

References

[1] Compton A H 1923 *Phys. Rev.* **22** 409
[2] Klein O and Nishina Y 1929 *Z. Phys.* **52** 853
[3] Ting A, Fischer R, Fisher A, Evans K, Burris R, Krall J, Esarey E and Sprangle P 1995 *J. Appl. Phys.* **78** 575
[4] Ting A, Fischer R, Fisher A, Moore C I, Hafizi B, Elton R, Krushelnick K, Burris R, Jackel S, Evans K, Weaver J N, Sprangle P, Esarey E, Baine M and Ride S 1996 *Nucl. Instrum. Methods Phys. Res. Sect. A* **375** ABS68
[5] Leemans W P, Schoenlein R W, Volfbeyn P, Chin A H, Glover T E, Balling P, Zolotorev M, Kim K J, Chattopadhyay S and Shank C V 1996 *Phys. Rev. Lett.* **77** 4182
[6] Pogorelsky I V, Ben-Zvi I, Hirose T, Kashiwagi S, Yakimenko V, Kusche K, Siddons P, Skaritka J, Kumita T, Tsunemi A, Omori T, Urakawa J, Washio M, Yokoya K, Okugi T, Liu Y, He P and Cline D 2000 *Phys. Rev. ST Accel. Beams* **3** 090702
[7] Sakai I, Aoki T, Dobashi K, Fukuda M, Higurashi A, Hirose T, Iimura T, Kurihara Y, Okugi T, Omori T, Urakawa J, Washio M and Yokoya K 2003 *Phys. Rev. ST Accel. Beams* **6** 091001
[8] Di Piazza A, Müller C, Hatsagortsyan K Z and Keitel C H 2012 *Rev. Mod. Phys.* **84** 1177
[9] Bula C, McDonald K T, Prebys E J, Bamber, C, Boege S, Kotseroglou T, Melissinos A C, Meyerhofer D D, Ragg W, Burke D L, Field R C, Horton-Smith G, Odian A C, Spencer J E, Walz D, Berridge S C, Bugg W M, Shmakov K and Weidemann A W 1996 *Phys. Rev. Lett.* **76** 3116
[10] Narozhny N B, Nikishov A I and Ritus V I 1965 *Sov. Phys. JETP* **20** 622
[11] Yanovsky V, Chvykov V, Kalinchenko G, Rousseau P, Planchon T, Matsuoka T, Maksimchuk A, Nees J, Cheriaux G, Mourou G and Krushelnick K 2008 *Opt. Express* **16** 2109
[12] Xie S Y, Lu Y F, Ma Q L, Wang P Y, Shen Y, Zong N, Yang F, Bo Y, Peng Q J, Cui D F and Xu Z Y 2010 *Chin. Phys. B* **19** 064208
[13] Schwinger J 1951 *Phys. Rev.* **82** 664
[14] Jiang M, Xie B S, Sang H B and Li Z L 2013 *Chin. Phys. B* **22** 100307
[15] Brown L S and Kibble T W B 1964 *Phys. Rev.* **133** A705
[16] Goldman I I 1964 *Sov. Phys. JETP* **46** 1412
[17] Nikishov A I and Ritus V I 1964 *Sov. Phys. JETP* **19** 529
[18] Zeldovich Y B 1975 *Sov. Phys. Usp.* **18** 79
[19] Baier V N, Katkov V M, Milstein A I and Strakhovenko V M 1976 *Sov. Phys. JETP* **42** 400
[20] Ivanov D Y, Kotkin G L and Serbo V G 2004 *Eur. Phys. J. C* **36** 127
[21] Mackenroth F and Di Piazza A 2011 *Phys. Rev. A* **83** 032106
[22] Mackenroth F and Di Piazza A 2013 *Phys. Rev. A* **87** 033401
[23] Kang H, Quan W and Lin Z 2010 *Phys. Rev. Lett.* **104** 203001
[24] Volkov D M 1935 *Z. Phys.* **94** 250
[25] Furry W H 1951 *Phys. Rev.* **81** 115
[26] Müller C, Hatsagortsyan K Z and Keitel C H 2008 *Phys. Rev. A* **78** 033408
[27] Müller C, Hatsagortsyan K Z and Keitel C H 2006 *Phys. Rev. D* **74** 074017
[28] Greiner W and Reinhardt J 2009 *Quantum Electrodynamics* (Berlin: Springer Press)
[29] Salamin Y I and Faisal F H M 1996 *Phys. Rev. A* **54** 4383
[30] Boca M and Florescu V 2010 *Romanian Journal in Physics* **55** 5
[31] Reiss H R 1962 *J. Math. Phys.* **3** 59
[32] Dattoli G, Chiccoli C and Lorenzutta S 1994 *Math. Anal. Appl.* **184** 201